Long Noncoding RNA PVT1 Silencing Prevents the Development of Uveal Melanoma by Impairing MicroRNA-17-3p–Dependent MDM2 Upregulation

Shuai Wu, Han Chen, Ning Han, Chunxia Zhang, and Hongtao Yan

Department of Ophthalmology, The Second Hospital of Jilin University, Changchun, People's Republic of China

Correspondence: Hongtao Yan, Department of Ophthalmology, The Second Hospital of Jilin University, No. 218, Ziqing Street, Nanguan District, Changchun 130000, Jilin Province, People's Republic of China;
yhtyanhongtao@126.com.

Submitted: June 5, 2019
Accepted: October 12, 2019

Citation: Wu S, Chen H, Han N, Zhang C, Yan H. Long noncoding RNA PVT1 silencing prevents the development of uveal melanoma by impairing microRNA-17-3p–dependent MDM2 upregulation. *Invest Ophthalmol Vis Sci*. 2019;60:4904–4914. https://doi.org/10.1167/iovs.19-27704

Purpose. Uveal melanoma is a common primary intraocular malignancy accompanied by high mortality. Previous evidence has highlighted the implication of microRNAs (miRNAs) and long noncoding RNAs (lncRNAs) in uveal melanoma. Accordingly, we further uncovered the possible role of lncRNA plasmacytoma variant translocation 1 gene (*PVT1*) and microRNA-17-3p (miR-17-3p) in uveal melanoma.

Methods. A series of experiments were performed to examine the relationship among lncRNA PVT1, miR-17-3p, and murine double minute clone 2 oncoprotein (MDM2). Afterward, gain- and loss-of-function approaches were used with uveal melanoma cells to verify the role of lncRNA PVT1, miR-17-3p, and MDM2 in the tumorigenesis and development of uveal melanoma.

Results. Highly expressed lncRNA PVT1 and MDM2, yet lowly expressed miR-17-3p, were identified in ocular uveal melanoma tissues versus normal adjacent tissues. Then, dual luciferase reporter gene assay, RNA binding protein immunoprecipitation, and RNA pull-down assays showed that lncRNA PVT1 specifically bound to miR-17-3p, and that *MDM2* was a target gene of miR-17-3p. Gain- and loss-of-function studies elucidated that silencing of lncRNA PVT1 or overexpression of miR-17-3p resulted in decreased MDM2 expression and increased transcriptional activity of p53, in addition to inhibiting uveal melanoma cell proliferation, migration, and invasion, yet promoted cell apoptosis in vitro. In addition, lncRNA PVT1 silencing or miR-17-3p overexpression was noted to inhibit tumor growth in vivo.

Conclusions. Downregulation of lncRNA PVT1 could potentially promote miR-17-3p expression to suppress tumorigenesis and development of uveal melanoma by activating the p53 signaling pathway through binding to MDM2.

Keywords: long noncoding RNA plasmacytoma variant translocation 1 gene, microRNA-17-3p, murine double minute clone 2 oncoprotein, p53, uveal melanoma

Uveal melanoma is a primary intraocular tumor that occurs owing to melanocytes residing in the stroma.[1] Uveal melanoma often forms undetectable micrometastases prior to diagnosis, which subsequently multiply to develop metastatic tumors, resulting in resistance to therapies.[2] Metastasis is a defining characteristic of uveal melanoma and is the main contributor to the high mortality seen in patients.[3] In recent years, the local control of the tumor has been an effective option in the treatment of uveal melanoma; however, half of these patients end up with advanced metastatic disease within 15 years.[4]

Long noncoding RNAs (lncRNAs) have been shown to play a role in the initiation and growth of the tumor owing to their ability to regulate chromatin organization, transcription, and posttranscription by modulating protein molecules, DNA, RNA, and/or their combinations.[5] In this study, the involvement of lncRNA plasmacytoma variant translocation 1 gene (*PVT1*) and microRNA-17-3p (miR-17-3p) in uveal melanoma tumorigenesis and development, and the underlying mechanism, were investigated. LncRNA PVT1 is a kind of lncRNA mapped to chromosome 8q24 and its copy-number amplification is a common event in malignant disease development.[6] LncRNA PVT1 expression is positively related to the risk of metastasis in primary uveal melanoma.[7] Our study revealed that there is a specific binding region between the lncRNA PVT1 sequence and the miR-17-3p sequence, and lncRNA PVT1 may downregulate expression of miR-17-3p, as determined by an online analysis software. MicroRNAs (miRNAs or miRs) have been extensively reported to be potential diagnostic and prognostic biomarkers in melanoma.[8] Uveal melanoma cell lines and tissues exhibit poor expression of several miRNAs, such as miR-145 and miR-224-5p, and their overexpression can suppress migration, proliferation, and cell cycle of uveal melanoma cells.[9,10] miRNAs contain 18 to 24 nucleotides and are known to target more than one-third of human mRNAs, regulating the target gene expression.[11] The results from in silico analysis have verified murine double minute clone 2 oncoprotein gene (*MDM2*) as a target gene of miR-17-3p. MDM2, encoded by the human homologue of the mouse double minute 2 gene, is a kind of oncoprotein that is upregulated in multiple cancers.[12,13] MDM2 has been reported to be negatively controlled by p53, which thereby contributes to proapoptotic gene transcription in uveal melanoma.[14] Our study was conducted with the main objective of elucidating the potential functional relevance of the PVT1/miR-17-3p/MDM2 network in the initiation and progression of uveal melanoma.

Table. Primer Sequences for RT-qPCR

Gene	Forward Sequence (5′-3′)	Reverse Sequence (5′-3′)
PVT1	TCTGGGGAATAACGCTGGTG	CAGCCACAGCCTCCCTTAAA
miR-17-3p	ACACTCCAGCTGGGACTGCAGTGAAGGCAC	TGGTGTCGTGGAGTCG
MDM2	GAATCATCGGACTCAGGTACATC	TCTGTCTCACTAATTGCTCTCCT
p53	CAGCACATGACGGAGGTTGT	TCATCCAAATACTCCACACGC
p21	TGTCCGTCAGAACCCATGC	AAAGTCGAAGTTCCATCGCTC
U6	CTCGCTTCGGCAGCACA	AACGCTTCACGAATTTGCGT
GADPH	GGAGCGAGATCCCTCCAAAAT	GGCTGTTGTCATACTTCTCATGG

Materials and Methods

Ethics Statement

The study was conducted with the approval of the Ethics Committee of The Second Hospital of Jilin University. Informed written consent was obtained from each participant prior to the study following the Declaration of Helsinki. The animal experiment strictly adhered to the *Guide for the Care and Use of Laboratory Animals* published by the National Institutes of Health and adhered to the ARVO Statement for the Use of Animals in Ophthalmic and Vision Research to minimize the pain, suffering, and discomfort to experimental animals.

Study Subjects

Uveal melanoma tissues were collected from 28 uveal melanoma patients at The Second Hospital of Jilin University from July 2016 to April 2018, along with 12 control samples of uveal tissues. Ocular uveal melanoma tissues and matched adjacent normal tissues (choroidal tissue), which were confirmed through histopathologic findings, were collected and stored in liquid nitrogen for subsequent analyses.[15]

Cell Culture

Four common human melanoma cell lines, namely, OCM-1A, MUM-2C, C918, and MUM-2B, were purchased from the Cell Bank of Chinese Academy of Sciences (Shanghai, China) (http://www.cellbank.org.cn). Human uveal melanocytes (UMs) were obtained from American Type Culture Collection. After recovery, OCM-1A, MUM-2C, C918, and MUM-2B cells were cultured in Roswell Park Memorial Institute (RPMI) 1640 (GIBCO-BRL, Invitrogen, Mt Waverly, VIC, Australia) containing 10% fetal bovine serum (FBS), 100 U/mL penicillin, and 100 mg/mL streptomycin, and UMs were cultured in FIC (Invitrogen, Carlsbad, CA, USA) containing 10% FBS, 100 U/mL penicillin, and 100 mg/mL streptomycin at 37°C with 5% CO_2. When cell confluence reached 90%, subculture was carried out. Afterward, two cell lines with much higher lncRNA PVT1 expression were screened by reverse transcription–quantitative polymerase chain reaction (RT-qPCR) for subsequent experiments.

RNA Isolation and RT-qPCR

The total RNA was extracted by Trizol (15596026; Invitrogen, Carlsbad, CA, USA) and the concentration and purity were measured by a Nano-Drop ND-1000 spectrophotometer (Nano-Drop Technologies, Wilmington, DE, USA). Next, 1 μg total RNA was reverse transcribed into complementary DNA according to a PrimeScript RT reagent Kit (RR047A; Takara Bio, Inc., Otsu, Shiga, Japan) and TaqMan MicroRNA Reverse Transcription Kit (Applied Biosystems, Inc., Foster City, CA, USA). The primers were designed and synthesized by Shanghai Sangon Biotechnology Co., Ltd. (Shanghai, China) (Table), based on the instructions provided on the EasyScript First-Strand cDNA Synthesis SuperMix (Cat. No. AE301-02; Beijing TransGen Biotech Co., Ltd., Beijing, China). Afterward, the products underwent RT-qPCR (SYBR Premix Ex TaqTM II; Takara Biotechnology Ltd., Dalian, China) using ABI 7500 FAST Real-Time PCR System (Applied Biosystems, Foster City, CA, USA). Relative expression of target genes was calculated by using the $2^{-\Delta\Delta Ct}$ method.[16]

Western Blot Analysis

The tissues or cells were resuspended in radioimmunoprecipitation assay (RIPA) lysis buffer (P0013B; Beyotime Biotechnology Co., Shanghai, China) containing phenylmethylsulfonyl fluoride and phosphatase inhibitor to isolate total protein. Afterward, the proteins were separated by sodium dodecyl sulfate–polyacrylamide gel electrophoresis and transferred onto nitrocellulose membranes. The membranes were blocked with 5% skim milk powder and incubation was carried out overnight at 4°C with the following primary antibodies purchased from Abcam, Inc. (Cambridge, UK): rabbit polyclonal antibody to MDM2 (1:1000, ab38618); p53 (1:1000, ab131442); p21 (1:1000, ab188224); and glyceraldehyde-3-phosphate dehydrogenase (GADPH) (1:2500, ab9485), which was used as a loading control. After being rinsed three times (15 min/time) with Tris-buffered saline Tween-20 (TBST) the following day, the membranes were incubated with horseradish peroxidase–labeled secondary goat anti-rabbit immunoglobulin G (IgG) (1:5000, ab205718) for 2 hours. Subsequently, the membranes were rinsed three times (15 min/time) with TBST again. The immunocomplexes on the membrane were visualized with enhanced chemiluminescence (ECL) solution and photographed by SmartView Pro 2000 (UVCI-2100; Major Science, Cambridge, MA, USA). The band intensities were quantified by using Quantity One software (Bio-Rad, Hercules, CA, USA).

Fluorescence In Situ Hybridization (FISH)

The cover glasses were placed at the bottom of a 24-well plate and the cells were inoculated at a density of 6×10^4 cells/well. When the cells reached 60% to 70% confluence, the cover glasses were removed. Next, the cells were fixed and permeabilized with pre-cold permeabilization buffer at 4°C for 5 minutes. Subsequently, prehybridization solution was added to the cells and blocked at 37°C for 30 minutes. Meanwhile, hybridization solution was preheated at 37°C. After the removal of prehybridization solution in each well, the cells were hybridized overnight with Stellaris RNA FISH (Biosearch Technologies, Novato, CA, USA) probe hybridization solution against lncRNA PVT1 probe at 37°C under dark conditions. Next, the cells were washed with wash solution I, II, and III at 42°C, and stained with 4′,6-diamidino-2-phenylindole (DAPI) for 10 minutes. The samples were then mounted and observed under a fluorescence microscope (Olympus, Tokyo, Japan).

Dual Luciferase Reporter Gene Assay

An online prediction software, RNA22 (https://cm.jefferson.edu/rna22/Precomputed/; available in the public domain), was used to predict target genes of miR-17-3p, which was further validated by dual luciferase reporter gene assay. Briefly, target site sequence (WT) of the 3′-untranslated region (UTR) of lncRNA PVT1 and MDM2 and site-directed mutation site (Mut) of the WT target site were synthesized. pmiR-RB-REPORT-PVT1-3′-UTR and pmiR-RB-REPORT-MDM2-3′-UTR plasmids (Guangzhou RiboBio Co., Ltd., Guangzhou, Guangdong, China) underwent restriction enzyme digestion. Subsequently, the artificially synthesized gene fragments WT and Mut were inserted into pmiR-RB-REPORT vectors (Guangzhou RiboBio) with the empty plasmids transfected as a control group. The correctly sequenced luciferase reporter plasmids WT and Mut were used for subsequent transfection for 48 hours. Afterward, relative fluorescence value was detected with the luciferase assay kit (RG005; Beyotime Biotechnology).[17]

RNA Binding Protein Immunoprecipitation (RIP) Assay

A RIP kit (Millipore, Billerica, MA, USA) was used to detect the binding between lncRNA PVT1, miR-17-3p, and Ago2 (binding to miRNA and required for RNA-mediated gene silencing [RNAi] by the RNA-induced silencing complex [RISC]). The OCM-1A cells were lysed with RIPA lysis buffer (P0013B; Beyotime Biotechnology) for 5 minutes. After centrifugation at 21,912.8*g* at 4°C for 10 minutes, one portion of the supernatant was taken as input, while the other portion was subjected to coprecipitation with antibody. Briefly, beads were resuspended in RIP wash buffer, after which 5 μg antibody was added for binding. Subsequently, the magnetic bead-antibody complex was resuspended and incubation was carried out at 4°C overnight with cell extract. The magnetic bead-protein complex was collected on a magnetic base. The sample and the input were digested with proteinase K, after which the RNA was extracted for subsequent RT-qPCR detection. The antibodies used in RIP assay included rabbit anti-human Ago2 (1:50, ab186733; Abcam), which was mixed for 30 minutes with rabbit anti-human IgG (1:100, ab109489; Abcam) used as negative control (NC).

RNA Pull-Down Assay

OCM-1A cells were transfected with 50 nM biotinylated WT-bio-miR-17-3p (wild-type miR-17-3p) and MUT-bio-miR-17-3p (mutant miR-17-3p, which cannot bind to lncRNA PVT1) (Wuhan GeneCreate Biological Engineering Co., Ltd., Hubei, China). After 48 hours, the cells were collected and lysed. The lysate was then incubated overnight at 4°C with beads (S3762; Sigma-Aldrich Chemical Company, St. Louis, MO, USA) pre-coated with RNase-free BSA and yeast tRNA at 4°C overnight. Subsequently, the cells were washed twice with precooled lysis buffer, three times with low-salt buffer, and once with high-salt buffer. Finally, the bound RNA was purified by Trizol, and RT-qPCR was conducted to detect the enrichment of lncRNA PVT1.

Cell Treatment

Recovered OCM-1A cells were cultured in 1640 culture medium containing 10% calf serum in 5% CO_2 at 37°C. The medium was changed at an interval of 3 days. OCM-1A cells at the logarithmic phase growth were selected. All target plasmids were purchased from Dharmacon (Lafayette, CO, USA). OCM-1A cells (3×10^5 cells/well) were seeded in a six-well plate and cultured in fresh complete medium. Afterward, the cells were transfected with the following plasmids, using a Lipofectamine 2000 kit (Invitrogen, Inc., Carlsbad, CA, USA): lncRNA PVT1 (pcDNA3.1-lncRNA PVT1), si-lncRNA PVT1 (pGPU6/Neo-lncRNA PVT1), miR-17-3p mimic, lncRNA PVT1 + miR-17-3p mimic (pcDNA3.1-lncRNA PVT1 + miR-17-3p mimic), miR-17-3p inhibitor, si-MDM2 (pGPU6/Neo-MDM2), and miR-17-3p inhibitor + si-MDM2 (miR-17-3p inhibitor + pGPU6/Neo-MDM2) as well as their corresponding controls (lncRNA PVT1 NC [pcDNA3.1], si-lncRNA PVT1 NC [pGPU6/Neo], miR-17-3p mimic NC, si-MDM2 NC [pGPU6/Neo], lncRNA PVT1 + miR-17-3p mimic NC, miR-17-3p inhibitor NC and si-MDM2 NC). The target plasmids pcDNA3.1 and pGPU6/Neo were purchased from Dharmacon Research, Inc., and Shanghai GenePharma Co., Ltd. (Shanghai, China). Subsequently, 4 μg target plasmids and 10 μL Lipofectamine 2000 were diluted by 250 μL serum-free Opti-MEM (Gibco, Carlsbad, CA, USA) medium, which was then allowed to stand for 5 minutes. The two were mixed well and left to stand for 30 minutes. Subsequently, the mixture was added to the wells and cultured in 5% CO_2 at 37°C for 6 hours. The cells were then further cultured for 48 hours.

Cell Counting Kit-8 (CCK-8) Assay

The cells were dispersed to make a single cell suspension by using a pipette. Next, the cells (2.5×10^3 cells/well) were seeded in a 96-well plate and cultured in 5% CO_2 at 37°C. Each group was repeated in three wells. A total of 10 μL CCK-8 reagent (CK04; Dojindo Laboratories, Kumamoto, Japan) was then added to each well after 24, 48, and 72 hours of culture, and then cultured for 2 hours in 5% CO_2 at 37°C. The optical density (OD) values were measured at 450 nm with an automated enzyme reader (Multiskan MK3; Thermo, Waltham, MA, USA). A cell growth curve was drawn with the average OD values of each group as abscissa (*x*-axis) and the time as ordinate (*y*-axis) in order to calculate cell viability.

Clonogenic Assay

The stably transfected OCM-1A cells (500 cells/well) were oscillated in a six-well plate and cultured in RPMI-1640 medium for 2 weeks. Afterward, 1% crystal violet (Beyotime Biotechnology) was used to stain the proliferating colony. Finally, the number of colonies was counted and colonies with ≥50 cells were photographed.

Annexin V-Fluorescein Isothiocyanate (FITC)/Propidium Iodide (PI) Double-Staining Assay

The apoptosis of OCM-1A cells after 24-hour culture was measured with the use of Annexin V-FITC/PI double-staining kit (556547; Shanghai Shuojia Biotechnology Co., Ltd., Shanghai, China). In short, after different centrifugations, OCM-1A cells were resuspended in 300 μL 1× binding buffer. Subsequently, Annexin V-FITC was added and incubation was carried out for 15 minutes. A total of 5 μL PI was added into the cells for 5-minute incubation in ice bath with the avoidance of light. Finally, a flow cytometer (Cube6; Partec, Muenster, Germany) was applied to detect FITC at the excitation wavelength of 480 nm and 530 nm, as well as PI at an excitation wavelength above 575 nm.

The serum in the cell culture medium was removed prior to cell transfection, after which cell cycle was synchronized by using serum starvation method. Afterward, cell transfection was conducted. Cells were prepared into a single cell suspension. Then, 70% precooled ethanol was added to the cells, which were fixed overnight at 4°C. Cells were

resuspended in 100 μL PBS and adjusted to a concentration of 1 mg/mL after the addition of RNase, followed by a water bath at 37°C for 30 minutes. Subsequently, PI staining solution was added to the cells to obtain a final concentration of 50 μg/mL, after which the cells were stained for 40 minutes at 4°C without light exposure. The DNA content was measured at a wavelength above 575 nm to calculate the percentage of cell cycle.

Scratch Test

A uniform horizontal line was drawn on the back of a six-well plate with a marker pen. Cells were then made into a single cell suspension and counted. Cells were seeded in a six-well plate at a density of 1×10^6 cells/well for 24 hours and then cultured in RPMI-1640 medium containing 10% FBS. A sterile 10-μL micropipette tip, which was perpendicular to the horizontal line on the back, was applied to make a scratch. The exfoliated cells induced by the pipette tip were removed, after which the cells were added with serum-free medium and cultured in 5% CO_2 at 37°C. Finally, the cells were observed and photographed under a microscope (Olympus) at 0 hours and 24 hours.

Transwell Assay

Thirty microliters of diluted Matrigel (1 mg/mL) was added to cover the apical chamber of Transwell chamber, followed by incubation for 4 hours at 37°C. Subsequently, the cell suspension (1×10^6 cells/mL) was inoculated. Next, the basolateral chamber was added with 700 μL RPMI-1640 medium containing 10% FBS, followed by incubation for 24 hours. Subsequently, the cells were fixed and stained with 0.05% crystal violet. Later, the chambers were rinsed with distilled water and the cells were gently wiped off in the basolateral chambers with a medical cotton ball. Finally, the invasive cells were photographed and counted under an inverted microscope (XSP-8CA; Shanghai Optical Instrument Factory, Shanghai, China).

Xenograft Tumor in Nude Mice

Thirty male BALB/c nude mice (aged 5 weeks, weighing 19–21 g; Shanghai Experimental Animal Center of the Chinese Academy of Sciences, Shanghai, China) were raised in a specific pathogen-free (SPF) grade environment with 12 hours of day/night cycle, constant temperature (25°C), and constant humidity (45%–50%), along with easily accessible sterile food and water. Next, mice were subcutaneously injected with an equal volume of OCM-1A cells (1×10^7 cells) treated with siRNA against PVT1 (si-LncRNA PVT1 group), NC of si-LncRNA PVT1 (si-LncRNA PVT1 NC group), miR-17-3p agomir (miR-17-3p agomir group), and miR-17-3p agomir NC (miR-17-3p agomir NC group) into the left axilla. Following successful inoculation, the tumor was observed every 5 days, and the long diameter (a) and short diameter (b) of the tumor were measured and recorded. The tumor volume was calculated with the following formula: Tumor Volume = $(a \times b^2)/2$. A tumor growth curve was then plotted. The nude mice were killed on the 35th day and the intact transplanted tumor was weighed.

Statistical Analysis

SPSS 21.0 statistical software (IBM Corp., Armonk, NY, USA) was used for data processing. The measurement data were described as mean ± standard deviation (SD). Data between two groups were compared with independent sample *t*-test. Comparisons among multiple groups were assessed by 1-way analysis of variance (ANOVA), followed by Tukey's post hoc tests. Data at different time points were compared by repeated measures ANOVA, followed by a Bonferroni post hoc test. P value < 0.05 was considered statistically significant.

Results

LncRNA PVT1 Silencing Impedes Biological Functions of Uveal Melanoma Cells

Initial RT-qPCR results depicted in Figures 1A and 1B showed higher lncRNA PVT1 expression in uveal melanoma tissues than in adjacent normal tissues ($P < 0.05$). Moreover, lncRNA PVT1 expression in OCM-1A, MUM-2C, C918, and MUM-2B cell lines was much higher than that observed in UMs (all $P < 0.05$), with OCM-1A and C918 cell lines having the highest lncRNA PVT1 expression. Therefore, OCM-1A and C918 cell lines were selected for subsequent experiments.

The subsequent findings from CCK-8, clonogenic assay (Figs. 1C–E), OCM-1A cell apoptosis and cell cycle (Figs. 1F–I), and scratch test and Transwell assay (Figs. 1J–M) revealed that OCM-1A cells transfected with lncRNA PVT1 showed an increase in S phase–arrested cells and in viability, invasion, and migration, while cell apoptosis, as well as G1 phase–arrested cells, was decreased ($P < 0.05$). However, si-lncRNA PVT1 transfection had opposite results with the aforementioned factors (all $P < 0.05$).

RT-qPCR and Western blot analysis verified that expression of miR-17-3p, p53, and p21 in OCM-1A cells transfected with lncRNA PVT1 was decreased, while MDM2 expression was increased ($P < 0.05$), the tendency of which was reversed upon si-lncRNA PVT1 transfection ($P < 0.05$) (Figs. 1N–P). In addition, all the aforementioned experiments were repeated in C918 cells. The findings suggested that all the results obtained from C918 cell lines were consistent with those from OCM-1A cell lines. These results showed that lncRNA PVT1 was overexpressed in uveal melanoma, and silencing of lncRNA PVT1 could result in the inhibition of proliferation, migration, and invasion of uveal melanoma cells.

LncRNA PVT1 Can Bind to miR-17-3p

RT-qPCR was conducted to detect the expression of miR-17-3p in UM, OCM-1A, MUM-2C, C918, and MUM-2B cell lines. The results showed upregulated expression of miR-17-3p in OCM-1A, MUM-2C, C918, and MUM-2B cell lines in comparison with that in UMs ($P < 0.05$) (Fig. 2A). An online prediction software, RNA22 (https://cm.jefferson.edu/rna22/Precomputed/; available in the public domain),[18] was used to determine that there is a binding site between lncRNA PVT1 and miR-17-3p, and miR-17-3p can target and bind to lncRNA PVT1 (Fig. 2B). The results of the dual luciferase reporter gene assay showed a significant decrease in luciferase activity of lncRNA PVT1 WT ($P < 0.05$), while that of lncRNA PVT1-MUT remained unaffected by miR-17-3p mimic transfection ($P > 0.05$) (Fig. 2C). As depicted in Figures 2E and 2F, the cells transfected with WT-miR-17-3p bound more lncRNA PVT1 than cells transfected with MUT-miR-17-3p and Bio-NC ($P < 0.05$), which further demonstrated that lncRNA PVT1 can bind with miR-17-3p. The results from FISH revealed that lncRNA PVT1 was localized at the cytoplasm (Fig. 2G).

As shown in Figures 2H and 2I, the expression of miR-17-3p, p53, and p21 was higher, and MDM2 expression was lower, in cells transfected with miR-17-3p mimic than in cells transfected with miR-17-3p mimic NC ($P < 0.05$). Expression of miR-17-3p, p53, and p21 was increased and MDM2 expression was decreased by lncRNA PVT1 + miR-17-3p mimic in contrast to lncRNA PVT1 + miR-17-3p mimic NC (all $P < 0.05$).

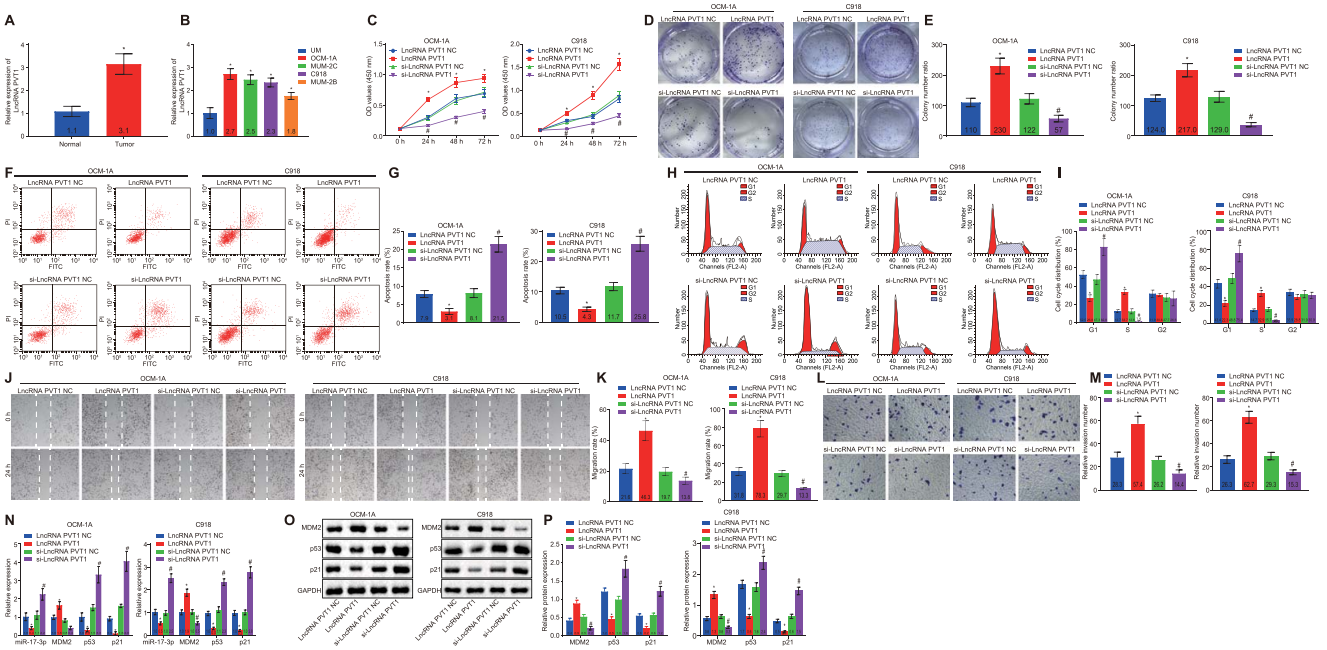

Figure 1. Silencing of lncRNA PVT1 inhibits the proliferation, migration, and invasion of uveal melanoma cells. The expression of lncRNA PVT1 in uveal melanoma tissues and matched adjacent normal tissues measured by RT-qPCR (**A**). The expression of lncRNA PVT1 in human UMs as well as uveal melanoma cell lines OCM-1A, MUM-2C, C918, and MUM-2B measured by RT-qPCR (**B**). The viability of cells transfected with lncRNA PVT1 and si-lncRNA PVT1 detected in CCK-8 assay (**C**). Colony formation in response to transfection of lncRNA PVT1 and si-lncRNA PVT1 (**D**, **E**). Cell apoptosis in response to transfection of lncRNA PVT1 and si-lncRNA PVT1 detected by flow cytometry (**F**, **G**). Cell cycle in response to transfection of lncRNA PVT1 and si-lncRNA PVT1 detected by flow cytometry (**H**, **I**). Cell migration in response to transfection of lncRNA PVT1 and si-lncRNA PVT1 measured by scratch test (**J**, **K**). Cell invasion in response to transfection of lncRNA PVT1 and si-lncRNA PVT1 measured by Transwell assay (**L**, **M**). The expression of miR-17-3p, MDM2, p53, and p21 in response to transfection of lncRNA PVT1 and si-lncRNA PVT1 measured by RT-qPCR (**N**). Western blot analysis of p21, p53, and MDM2 proteins in response to transfection of lncRNA PVT1 and si-lncRNA PVT1, which was normalized to GAPDH (**O**, **P**). $^{*}P < 0.05$ versus cells transfected with lncRNA PVT1 NC, $\#P < 0.05$ versus cells transfected with si-lncRNA PVT1 NC. Data (mean ± SD) between two groups were analyzed by using unpaired *t*-test, while those at different time points were compared by repeated measures ANOVA, followed by a Bonferroni post hoc test. The experiment was repeated in triplicate.

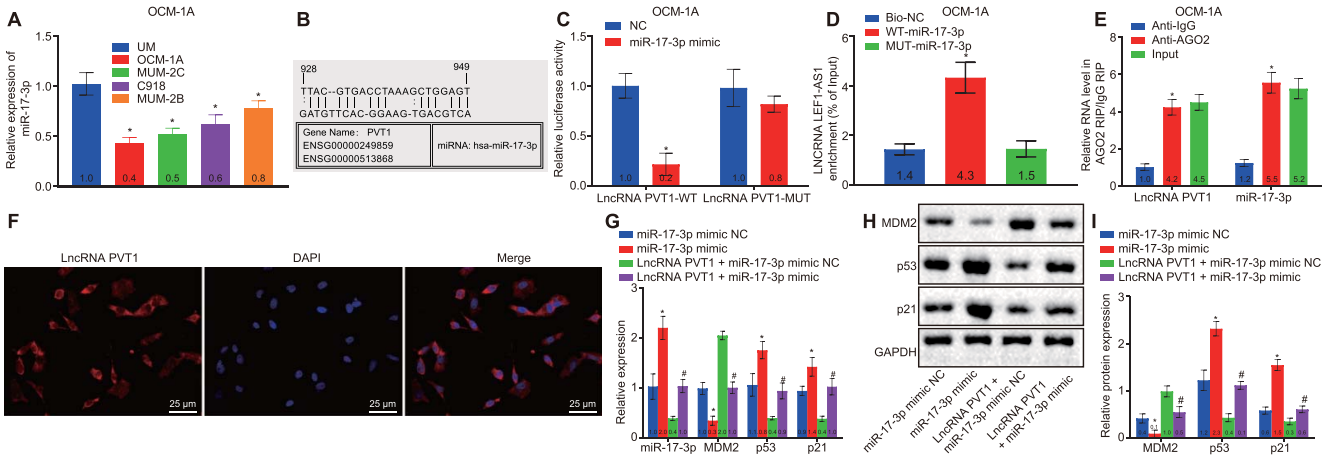

Figure 2. LncRNA PVT1 can bind to miR-17-3p. The expression of miR-17-3p in UM, OCM-1A, MUM-2C, C918, and MUM-2B cell lines detected by RT-qPCR (**A**). The binding site between miR-17-3p and lncRNA PVT1 predicted by using online software RNA22 (https://cm.jefferson.edu/rna22/Precomputed/; provided in the public domain) (**B**). The binding of miR-17-3p to lncRNA PVT1 confirmed by dual luciferase reporter gene assay (**C**). $^{*}P < 0.05$ versus cells transfected with NC. The binding of miR-17-3p to lncRNA PVT1 analyzed by RNA pull-down assay (**D**). The binding of lncRNA PVT1 to Ago2 detected by RIP assay (**E**). $^{*}P < 0.05$ versus cells transfected with IgG. Subcellular localization of lncRNA PVT1 (×400) revealed by FISH (**F**). Expression of miR-17-3p, MDM2, p53, and p21 in response to miR-17-3p mimic and lncRNA PVT1 + miR-17-3p mimic transfection detected by RT-qPCR (**G**). Western blot analysis of p21, p53, and MDM2 proteins, which was normalized to GAPDH in response to miR-17-3p mimic and lncRNA PVT1 + miR-17-3p mimic transfection (**H**, **I**). $^{*}P < 0.05$ versus cells transfected with miR-17-3p mimic NC, $\#P < 0.05$ versus cells transfected with lncRNA PVT1 + miR-17-3p mimic NC. Data (mean ± SD) were analyzed by unpaired *t*-test and those at different time points were compared by repeated measures ANOVA, followed by a Bonferroni post hoc test. The experiment was repeated in triplicate.

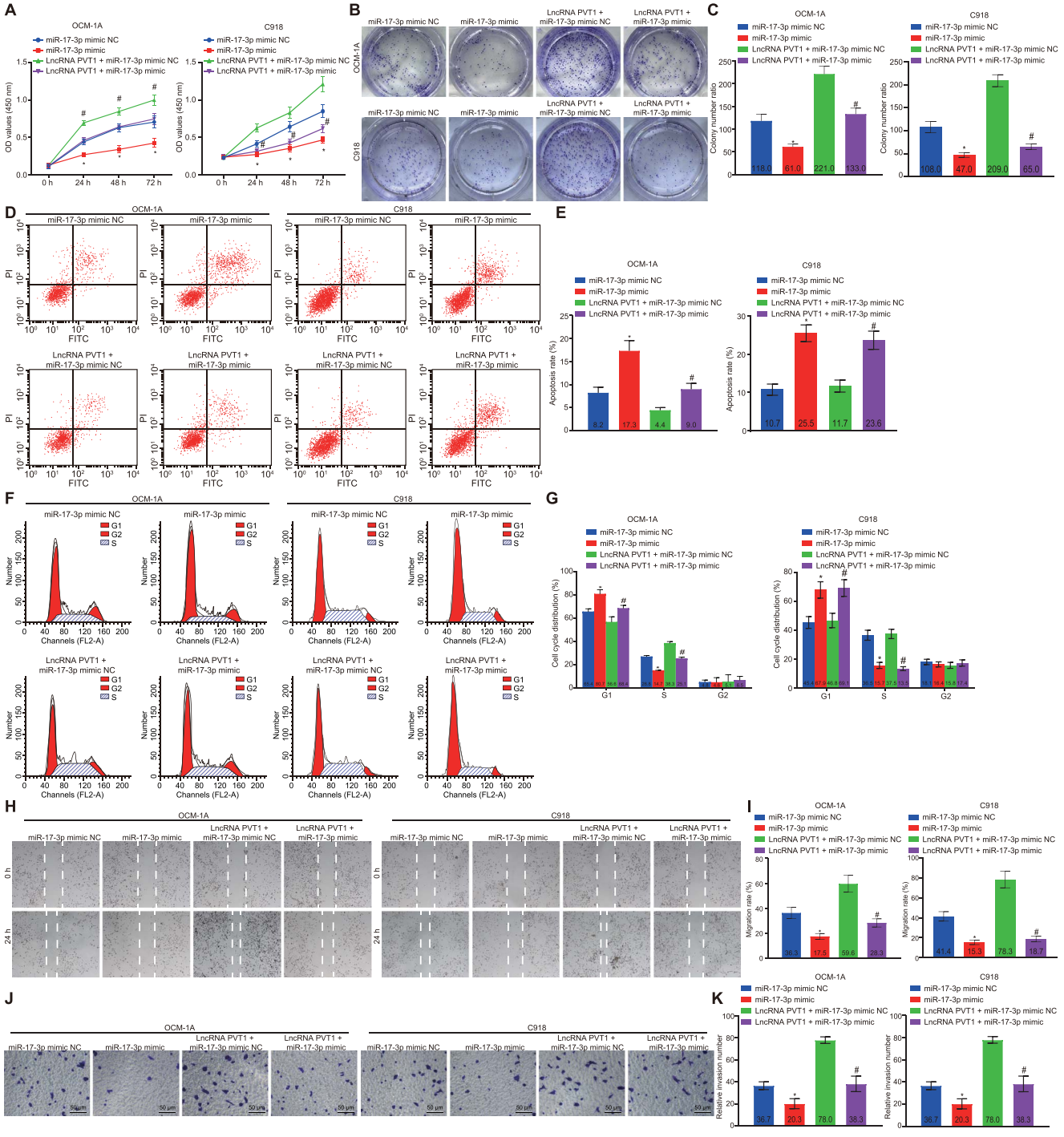

FIGURE 3. LncRNA PVT1 promotes proliferation, migration, and invasion of uveal melanoma cells. Cells were transfected with miR-17-3p mimic NC, miR-17-3p mimic, lncRNA PVT1 + miR-17-3p mimic, and lncRNA PVT1 + miR-17-3p mimic NC. The viability of cells in response to different transfections detected in CCK-8 assay (**A**). Colony formation in response to different transfections (**B**, **C**). Cell apoptosis in response to different transfections detected by flow cytometry (**D**, **E**). Cell cycle in response to different transfections detected by flow cytometry (**F**, **G**). Cell migration in response to different transfections (**H**, **I**). Cell invasion in response to different transfections (**J**, **K**). *$P < 0.05$ versus cells without any treatment, #$P < 0.05$ versus cells transfected with lncRNA PVT1 + miR-17-3p mimic NC. Data (mean ± SD) at different time points were compared by repeated measures ANOVA followed by a Bonferroni post hoc test, while those among multiple groups were assessed by 1-way ANOVA followed by Tukey's post hoc tests. The experiment was repeated in triplicate.

LncRNA PVT1 Promotes Biological Functions of Uveal Melanoma Cells via miR-17-3p

To determine whether miR-17-3p mediated the effect of lncRNA PVT1 on uveal melanoma cells, we altered the expression of miR-17-3p and lncRNA PVT1. The results showed a decrease in OCM-1A cell viability, invasion, and migration, and an increase in cell apoptosis, and G1 phase–arrested cells, while S phase–arrested cells were reduced upon miR-17-3p mimic transfection (all $P < 0.05$). Moreover, similar trends for these indicators were observed in OCM-1A cells transfected with lncRNA PVT1 + miR-17-3p mimic in contrast

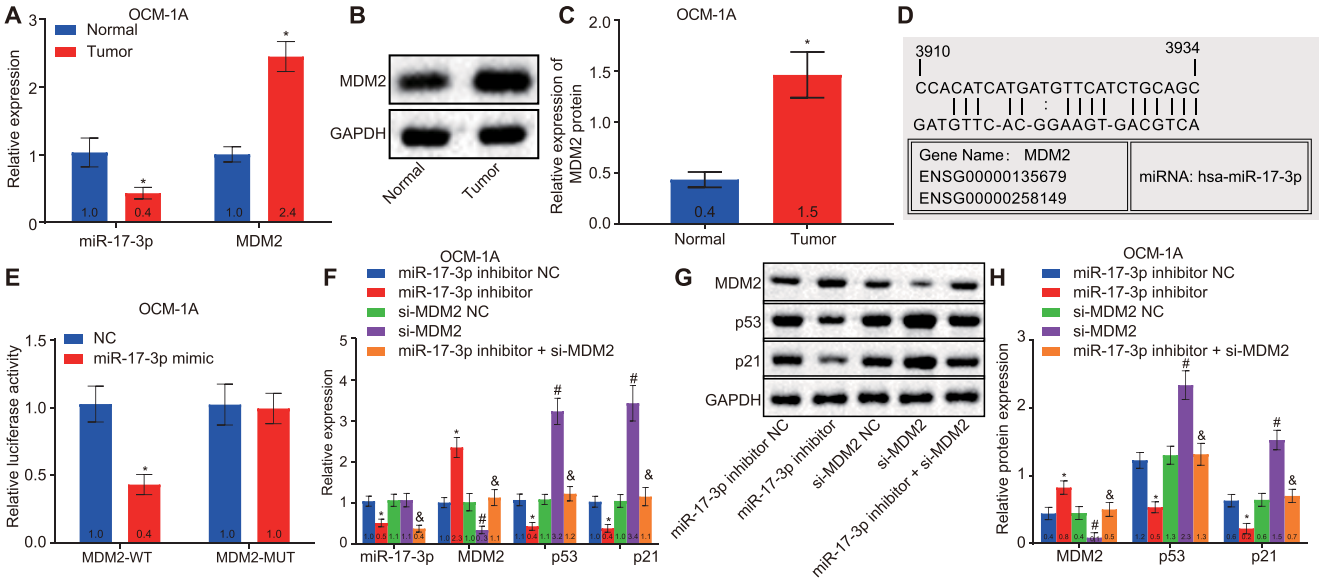

Figure 4. miR-17-3p facilitates the activation of p53 by inhibiting MDM2. Expression of miR-17-3p and MDM2 in uveal melanoma tissues and matched adjacent normal tissues measured by RT-qPCR (**A**). Western blot analysis of MDM2 protein in uveal melanoma tissues and matched adjacent normal tissues, which was normalized to GAPDH (**B**, **C**). The binding site between miR-17-3p and MDM2 predicted by using online software RNA22 (https://cm.jefferson.edu/rna22/Precomputed/; available in the public domain) (**D**). The binding of miR-17-3p to MDM2 confirmed by dual luciferase reporter gene assay (**E**). $^*P < 0.05$ versus cells transfected with NC. Expression of miR-17-3p, MDM2, p53, and p21 in response to miR-17-3p inhibitor, miR-17-3p inhibitor NC, si-MDM2, si-MDM2 NC, and miR-17-3p inhibitor + si-MDM2 transfection measured by RT-qPCR (**F**). Western blot analysis of p21, p53, and MDM2 proteins in response to miR-17-3p inhibitor, miR-17-3p inhibitor NC, si-MDM2, si-MDM2 NC, and miR-17-3p inhibitor + si-MDM2 transfection, which was normalized to GAPDH (**G**, **H**). $^*P < 0.05$ versus cells transfected with miR-17-3p inhibitor NC, $\#P < 0.05$ versus cells transfected with si-MDM2 NC, and $P < 0.05$ versus cells transfected with si-MDM2. Data (mean ± SD) at different time points were compared by the repeated measures ANOVA followed by a Bonferroni post hoc test, while those among multiple groups were assessed by 1-way ANOVA followed by Tukey's post hoc tests. The experiment was repeated in triplicate.

to lncRNA PVT1 + miR-17-3p mimic NC transfection (all $P < 0.05$) (Fig. 3). All of the above experiments were repeated in C918 cells. The findings suggested that all the results obtained from C918 cell lines were consistent with those from OCM-1A cell lines. These results suggest that lncRNA PVT1 could stimulate proliferation, invasion, and migration of uveal melanoma cells through the downregulation of miR-17-3p.

miR-17-3p Activates p53 by Targeting MDM2

Uveal melanoma tissues showed low miR-17-3p expression and high MDM2 expression ($P < 0.05$) (Figs. 4A–C). Moreover, there was a binding site between miR-17-3p and MDM2 (Fig. 4D). Dual luciferase reporter gene assay showed a remarkable decrease in luciferase activity following cotransfection of miR-17-3p and MDM2-WT ($P < 0.05$), while that following cotransfection of miR-17-3p and MDM2-MUT remained unaffected ($P > 0.05$) (Fig. 4E), suggesting a target relationship between miR-17-3p and MDM2.

Subsequent results from RT-qPCR and Western blot analysis showed that expression of miR-17-3p, p53, and p21 was decreased, while MDM2 expression was elevated in cells transfected with miR-17-3p inhibitor (all $P < 0.05$). The expression of miR-17-3p was decreased ($P < 0.05$), while the expression of MDM2, p53, and p21 did not change in cells transfected with miR-17-3p inhibitor + si-MDM2 ($P > 0.05$). There were no significant changes detected in the expression of miR-17-3p ($P > 0.05$), while p53 and p21 expression was higher and MDM2 expression was lower ($P < 0.05$) in cells treated with si-MDM2 (Figs. 4F–H). In comparison with cells treated with si-MDM2, the expression of miR-17-3p, p53, and p21 was reduced, while MDM2 expression was enhanced, in cells treated with miR-17-3p inhibitor + si-MDM2 ($P < 0.05$). The above results demonstrated that miR-17-3p can promote the activation of p53 by suppressing MDM2.

miR-17-3p Suppresses Viability, Migration, and Invasion of Uveal Melanoma Cells by Downregulating MDM2

Following miR-17-3p inhibitor transfection, OCM-1A cell viability (Figs. 5A–C), invasion (Figs. 5J, 5K), and migration (Figs. 5H, 5I) were increased, while cell apoptosis (Figs. 5D, 5E) was decreased with fewer cells at the G1 phase and more cells at the S phase (Figs. 5F, 5G) (all $P < 0.05$). No obvious changes were observed in relation to cell cycle, apoptosis, migration, and invasion of cells transfected with miR-17-3p inhibitor + si-MDM2 ($P > 0.05$). Moreover, transfection with si-MDM2 resulted in decreased cell viability, invasion, and migration, while apoptosis was increased with more G1 phase–arrested cells and fewer S phase–arrested cells when compared with cells transfected with si-MDM2 NC (all $P < 0.05$). In comparison with cells treated with si-MDM2, enhanced cell viability, invasion, and migration and more S phase–arrested cells were detected, while apoptosis was reduced and G1 phase–arrested cells were fewer in those cells treated with miR-17-3p inhibitor + si-MDM2 ($P < 0.05$). In addition, we repeated all the above-mentioned experiments in C918 cells. The findings suggested that all the results obtained from C918 cell lines were consistent with those from OCM-1A cell lines. The aforementioned findings indicated that overexpressed miR-17-3p can repress viability, migration, and invasion of uveal melanoma cells through MDM2 downregulation.

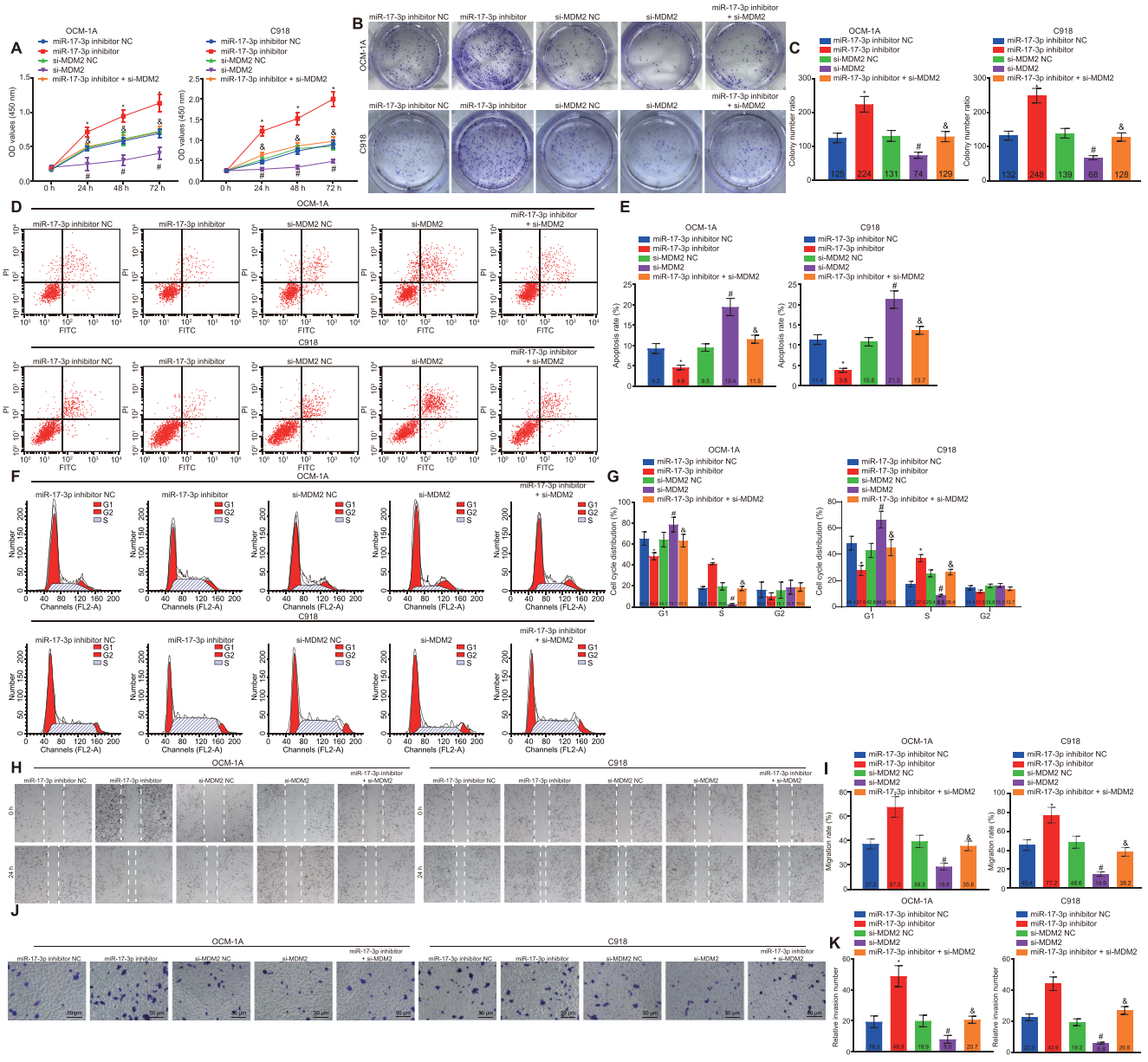

FIGURE 5. Overexpressed miR-17-3p represses viability, migration, and invasion of uveal melanoma cells by downregulating MDM2. Cells were transfected with miR-17-3p inhibitor, miR-17-3p inhibitor NC, si-MDM2, si-MDM2 NC, and miR-17-3p inhibitor + si-MDM2. The viability of cells with different transfections detected by CCK-8 assay (**A**). Colony formation in response to cells with different transfections (**B**, **C**). Cell apoptosis in response to different transfections detected by flow cytometry (**D**, **E**). Cell cycle in response to different transfections detected by flow cytometry (**F**, **G**). Cell migration in response to different transfections measured by scratch test (**H**, **I**). Cell invasion in response to different transfections detected by Transwell assay (**J**, **K**). $^{*}P < 0.05$ versus cells transfected with miR-17-3p inhibitor NC, $^{\#}P < 0.05$ versus cells transfected with si-MDM2 NC, and $P < 0.05$ versus cells transfected with si-MDM2. Data (mean ± SD) at different time points were compared by the repeated measures ANOVA followed by a Bonferroni post hoc test, while those among multiple groups were assessed by 1-way ANOVA followed by Tukey's post hoc tests. The experiment was repeated in triplicate.

LncRNA PVT1 Silencing or miR-17-3p Overexpression Reduces Tumorigenic Ability of Uveal Melanoma in Nude Mice by Restoring p3 and Reducing MDM2

As shown in Figure 6, the tumor volume and weight were smaller, the expression of miR-17-3p, p53, and p21 was higher, and MDM2 expression was lower in mice injected with cells expressing si-lncRNA PVT1 than in mice injected with cells expressing si-lncRNA PVT1 NC (all $P < 0.05$). Moreover, compared with mice injected with cells expressing miR-17-3p agomir NC, tumor volume and weight were decreased, expression of miR-17-3p, p53, and p21 was increased, and MDM2 expression was decreased in mice injected with cells expressing miR-17-3p agomir (all $P < 0.05$). Therefore, lncRNA PVT1 impaired miR-17-3p–mediated MDM2-p53 upregulation, thereby stimulating tumorigenic ability of uveal melanoma in vivo.

DISCUSSION

With a high risk of distant tumor spread, the metastatic feature of uveal melanoma usually causes high mortality.[3] Various lncRNAs have been reported to facilitate uveal melanoma

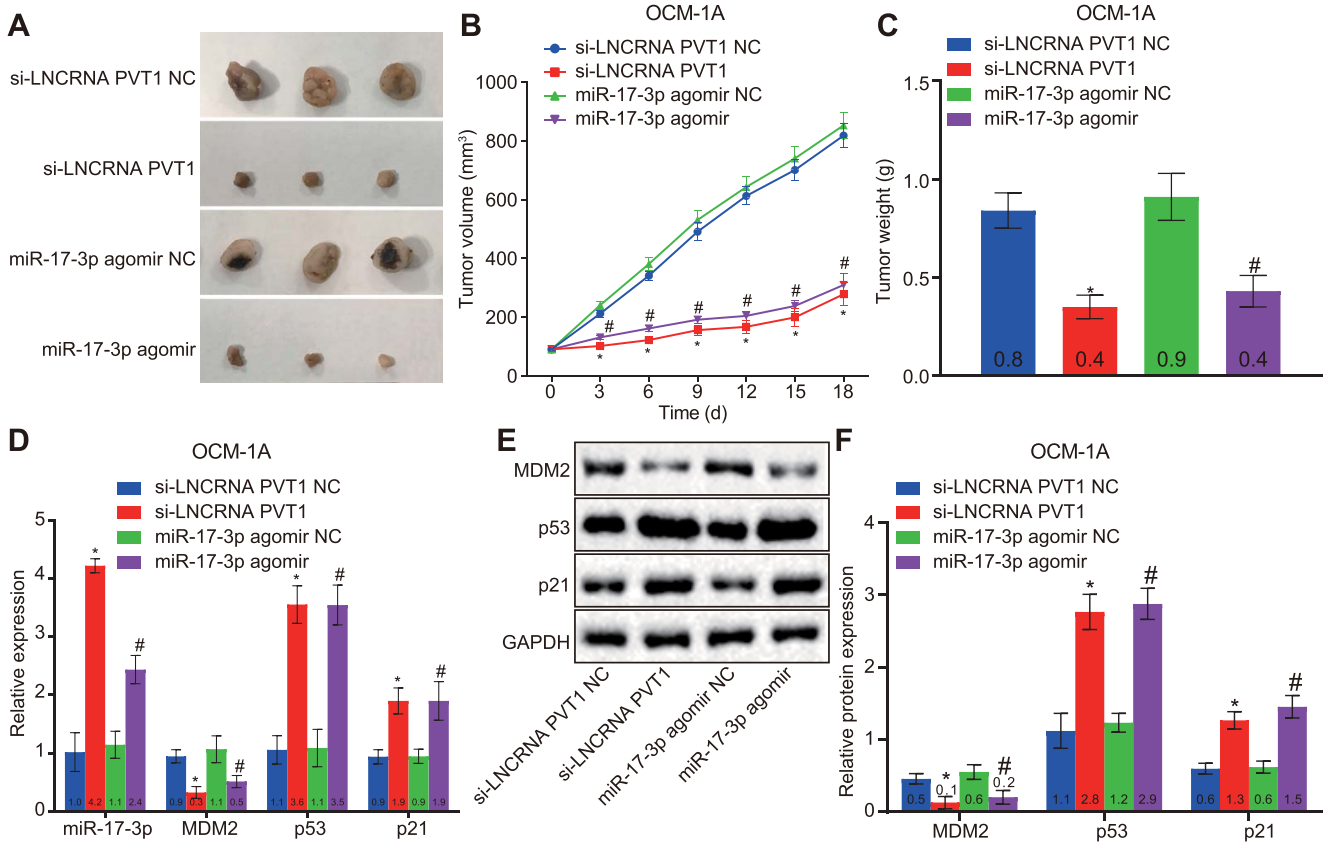

Figure 6. Silencing of lncRNA PVT1 or overexpressed miR-17-3p reduces the tumorigenic ability of uveal melanoma in nude mice. Xenograft tumors and quantitative analysis of tumor mass after injection with cells expressing si-lncRNA PVT1 and miR-17-3p agomir (**A**–**C**). The expression of miR-17-3p, MDM2, p63, and p21 after injection with cells expressing si-lncRNA PVT1 and miR-17-3p agomir detected by RT-qPCR (**D**). Western blot analysis of p21, p53, and MDM2 proteins after injection with cells expressing si-lncRNA PVT1 and miR-17-3p agomir, which was normalized to GAPDH (**E**, **F**). $^*P < 0.05$ versus mice injected with si-lncRNA PVT1 NC, $\#P < 0.05$ versus mice injected with miR-17-3p agomir NC. Data (mean ± SD) at different time points were compared by repeated measures ANOVA followed by a Bonferroni post hoc test, while those among multiple groups were assessed by 1-way ANOVA, followed by Tukey's post hoc tests. The experiment was repeated in triplicate.

development.[19,20] The experiments conducted in the present study demonstrated the mechanism by which lncRNA PVT1 is involved in uveal melanoma, which was found to be through the regulation of miR-17-3p and MDM2-p53. Collectively, our findings revealed that silencing of lncRNA PVT1 or overexpression of miR-17-3p can decrease MDM2 expression and increase p53 transcriptional activity, thereby inhibiting the tumorigenesis and development of uveal melanoma.

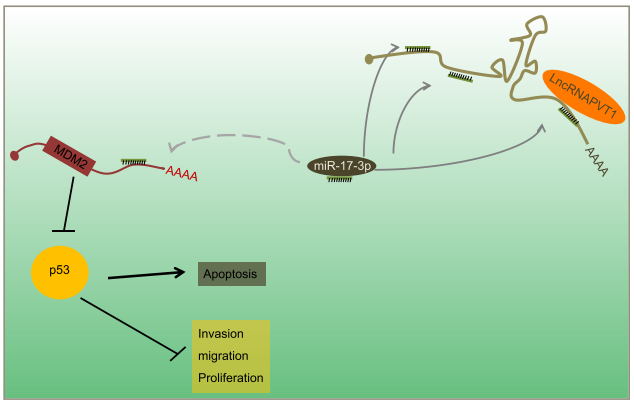

Figure 7. The schematic diagram depicts the PVT1/miR-17-3p/MDM2/p53 axis regulating the proliferation, migration, and invasion of uveal melanoma cells. LncRNA PVT1 promotes the proliferation, migration, and invasion of uveal melanoma cells while suppressing cell apoptosis by upregulating MDM2 and reducing p53 by binding to miR-17-3p.

Initially, uveal melanoma tissues presented with overexpressed lncRNA PVT1 and poorly expressed miR-17-3p. It has been reported that lncRNA PVT1 is often highly expressed in cancer cells and tissues and acts as an oncogenic lncRNA in uveal melanoma.[7] Multiple miRNAs, including miR-340b/c and miR-137, have poor expression in uveal melanoma cells, and in cases where there is an upregulation, these miRNAs play a suppressor role during the development of uveal melanoma.[21,22] Moreover, metastatic melanoma cell lines have low expression of miR-17-5p.[23] LncRNA PVT1 silencing transfection resulted in inhibited proliferation, migration, and invasion of uveal melanoma cells. Xu et al.[7] have found that overexpressed lncRNA PVT1 can independently predict a poor overall survival for patients with primary uveal melanoma, owing to the role lncRNA PVT1 plays as a carcinogenetic factor through a variety of epigenetic mechanisms, such as affecting transcription activity and regulating the expression of miRNAs, which are in line with our present findings.[7] Upregulated miR-17-5p could inhibit the aggressive behavior of the disease in melanoma by increasing posttranscriptional events and downregulating the expression of PD-L1.[23] The antitumor effects of miR-17 on melanoma have also been reported by Khorshidi et al.[24] Therefore, lncRNA PVT1 and miR-17-3p can be potential biological biomarkers of uveal melanoma diagnosis.

Furthermore, our study found that lncRNA PVT1 has a promoting effect on tumorigenesis and development of uveal melanoma by downregulating the expression of miR-17-3p, which subsequently promoted MDM2 expression and inactivation of p53. A previous study[25] has identified miR-33a as a target of an lncRNA, CCAT1, and the knockdown of CCAT1 could result in the significant upregulation in the expression of miR-33a, which acts to suppress the invasion, proliferation, and migration abilities of melanoma cells. Wei et al.[26] have revealed that UCA1 binds to miR-507 to promote cell cycle, proliferation, and invasion of melanoma cells. The target relationship between MDM2 and miR-17-3p has also been demonstrated in glioblastoma in a previously conducted study.[27] Furthermore, MDM2 is targeted and negatively regulated by miR-17-3p in gastric cancer cells.[28] Several studies have also demonstrated the regulatory function of the miR-17-3p/MDM2/p53 axis in several types of cancer, including melanoma.[29] miR-509-5p decreases the G1/S-phase transition of the cell cycle by targeting MDM2 and inhibits the migration, growth, and invasion of cancer cells in cervical cancer and hepatoma.[30] As reported previously, MDM2 is poorly expressed in many human cancers and plays an oncogenic role mainly by suppressing the antitumor ability of p53.[31,32] The aforementioned findings suggest that lncRNA PVT1 silencing might play a protective role against the development of uveal melanoma by upregulating miR-17-3p and activating the p-53 signaling pathway while decreasing MDM2 expression.

Conclusion

In conclusion, lncRNA PVT1 can upregulate MDM2 by binding to miR-17-3p, thus aggravating uveal melanoma (Fig. 7). The function of lncRNA PVT1 in uveal melanoma was further explored in our study at the cellular and animal levels, the results of which suggested that lncRNA PVT1 regulates MDM2 expression by binding to miR-17-3p, ultimately affecting the occurrence and development of uveal melanoma through p53. The results of this study clarify the function of lncRNA PVT1 in uveal melanoma and its molecular mechanism, and it has the potential to be used as a candidate molecular marker of uveal melanoma. Investigation of the PVT1/miR-17-3p/MDM2-p53 network in uveal melanoma yields a better understanding of its in-depth mechanisms and may have potentially important therapeutic implications in the treatment of uveal melanoma.

Acknowledgments

The authors thank all participants enrolled in the present study.

Disclosure: **S. Wu**, None; **H. Chen**, None; **N. Han**, None; **C. Zhang**, None; **H. Yan**, None

References

1. Spagnolo F, Caltabiano G, Queirolo P. Uveal melanoma. *Cancer Treat Rev*. 2012;38:549–553.
2. Onken MD, Worley LA, Tuscan MD, Harbour JW. An accurate, clinically feasible multi-gene expression assay for predicting metastasis in uveal melanoma. *J Mol Diagn*. 2010;12:461–468.
3. Harbour JW, Onken MD, Roberson ED, et al. Frequent mutation of BAP1 in metastasizing uveal melanomas. *Science*. 2010;330:1410–1413.
4. Kashyap S, Meel R, Singh L, Singh M. Uveal melanoma. *Semin Diagn Pathol*. 2016;33:141–147.
5. Yang G, Lu X, Yuan L. LncRNA: a link between RNA and cancer. *Biochim Biophys Acta*. 2014;1839:1097–1109.
6. Takahashi Y, Sawada G, Kurashige J, et al. Amplification of PVT-1 is involved in poor prognosis via apoptosis inhibition in colorectal cancers. *Br J Cancer*. 2014;110:164–171.
7. Xu H, Gong J, Liu H. High expression of lncRNA PVT1 independently predicts poor overall survival in patients with primary uveal melanoma. *PLoS One*. 2017;12:e0189675.
8. Latchana N, Ganju A, Howard JH, Carson WE III. MicroRNA dysregulation in melanoma. *Surg Oncol*. 2016;25:184–189.
9. Li Y, Huang Q, Shi X, et al. MicroRNA 145 may play an important role in uveal melanoma cell growth by potentially targeting insulin receptor substrate-1. *Chin Med J (Engl)*. 2014;127:1410–1416.
10. Zheng X, Tang H, Zhao X, Sun Y, Jiang Y, Liu Y. Long noncoding RNA FTH1P3 facilitates uveal melanoma cell growth and invasion through miR-224-5p. *PLoS One*. 2017;12:e0184746.
11. Farazi TA, Spitzer JI, Morozov P, Tuschl T. miRNAs in human cancer. *J Pathol*. 2011;223:102–115.
12. Zhang X, Miao X, Guo Y, et al. Genetic polymorphisms in cell cycle regulatory genes MDM2 and TP53 are associated with susceptibility to lung cancer. *Hum Mutat*. 2006;27:110–117.
13. Chang YS, Graves B, Guerlavais V, et al. Stapled alpha-helical peptide drug development: a potent dual inhibitor of MDM2 and MDMX for p53-dependent cancer therapy. *Proc Natl Acad Sci U S A*. 2013;110:E3445–E3454.
14. Davies L, Spiller D, White MR, Grierson I, Paraoan L. PERP expression stabilizes active p53 via modulation of p53-MDM2 interaction in uveal melanoma cells. *Cell Death Dis*. 2011;2:e136.
15. Leung TW, Tang AM, Zee B, et al. Construction of the Chinese University Prognostic Index for hepatocellular carcinoma and comparison with the TNM staging system, the Okuda staging system, and the Cancer of the Liver Italian Program staging system: a study based on 926 patients. *Cancer*. 2002;94:1760–1769.
16. Arocho A, Chen B, Ladanyi M, Pan Q. Validation of the 2-DeltaDeltaCt calculation as an alternate method of data analysis for quantitative PCR of BCR-ABL P210 transcripts. *Diagn Mol Pathol*. 2006;15:56–61.
17. Collin SP. Topographic organization of the ganglion cell layer and intraocular vascularization in the retinae of two reef teleosts. *Vision Res*. 1989;29:765–775.
18. Miranda KC, Huynh T, Tay Y, et al. A pattern-based method for the identification of MicroRNA binding sites and their corresponding heteroduplexes. *Cell*. 2006;126:1203–1217.
19. Lu L, Yu X, Zhang L, et al. The long non-coding RNA RHPN1-AS1 promotes uveal melanoma progression. *Int J Mol Sci*. 2017;18:226.
20. Sun L, Sun P, Zhou QY, Gao X, Han Q. Long noncoding RNA MALAT1 promotes uveal melanoma cell growth and invasion by silencing of miR-140. *Am J Transl Res*. 2016;8:3939–3946.
21. Dong F, Lou D. MicroRNA-34b/c suppresses uveal melanoma cell proliferation and migration through multiple targets. *Mol Vis*. 2012;18:537–546.
22. Chen X, Wang J, Shen H, et al. Epigenetics, microRNAs, and carcinogenesis: functional role of microRNA-137 in uveal melanoma. *Invest Ophthalmol Vis Sci*. 2011;52:1193–1199.
23. Audrito V, Serra S, Stingi A, et al. PD-L1 up-regulation in melanoma increases disease aggressiveness and is mediated through miR-17-5p. *Oncotarget*. 2017;8:15894–15911.
24. Khorshidi A, Dhaliwal P, Yang BB. Anti-tumor activity of miR-17 in melanoma. *Cell Cycle*. 2015;14:2549–2550.
25. Lv L, Jia JQ, Chen J. The lncRNA CCAT1 upregulates proliferation and invasion in melanoma cells via suppressing miR-33a. *Oncol Res*. 2018;26:201–208.

Investigative Ophthalmology & Visual Science

26. Wei Y, Sun Q, Zhao L, et al. LncRNA UCA1-miR-507-FOXM1 axis is involved in cell proliferation, invasion and G0/G1 cell cycle arrest in melanoma. *Med Oncol*. 2016;33:88.
27. Li H, Yang BB. Stress response of glioblastoma cells mediated by miR-17-5p targeting PTEN and the passenger strand miR-17-3p targeting MDM2. *Oncotarget*. 2012;3:1653–1668.
28. Wang M, Gu H, Qian H, et al. miR-17-5p/20a are important markers for gastric cancer and murine double minute 2 participates in their functional regulation. *Eur J Cancer*. 2013; 49:2010–2021.
29. Kim E, Shohet J. Targeted molecular therapy for neuroblastoma: the ARF/MDM2/p53 axis. *J Natl Cancer Inst*. 2009;101: 1527–1529.
30. Ren ZJ, Nong XY, Lv YR, et al. Mir-509-5p joins the Mdm2/p53 feedback loop and regulates cancer cell growth. *Cell Death Dis*. 2014;5:e1387.
31. Wade M, Li YC, Wahl GM. MDM2, MDMX and p53 in oncogenesis and cancer therapy. *Nat Rev Cancer*. 2013;13: 83–96.
32. Araki S, Eitel JA, Batuello CN, et al. TGF-beta1-induced expression of human Mdm2 correlates with late-stage metastatic breast cancer. *J Clin Invest*. 2010;120:290–302.

Investigative Ophthalmology & Visual Science